Proteome Characterization of Glaucoma Aqueous Humor

Authors

Xiaoyan Liu, Xiang Liu, Ying Wang, Haidan Sun, Zhengguang Guo, Xiaoyue Tang, Jing Li, Xiaolian Xiao, Shuxin Zheng, Mengxi Yu, Chengyan He, Jiyu Xu, and Wei Sun

Correspondence

sunwei1018@sina.com

In Brief

Liu et al. characterized the proteome of aqueous humor from three types of glaucoma. Fifty-seven primary acute angle-closure glaucoma (PAACG), 50 primary chronic angle-closure glaucoma (PCACG), 35 neovascular glaucoma (NVG), and 33 cataract patient samples were analyzed using data-independent analysis and parallel reaction monitoring. Lipid metabolism, immune response, and cell death pathways showed different degrees of activation among the three types of glaucoma but were all higher relative to cataract. SERPIND1 was discovered as a vital protein in glaucoma.

Graphical Abstract

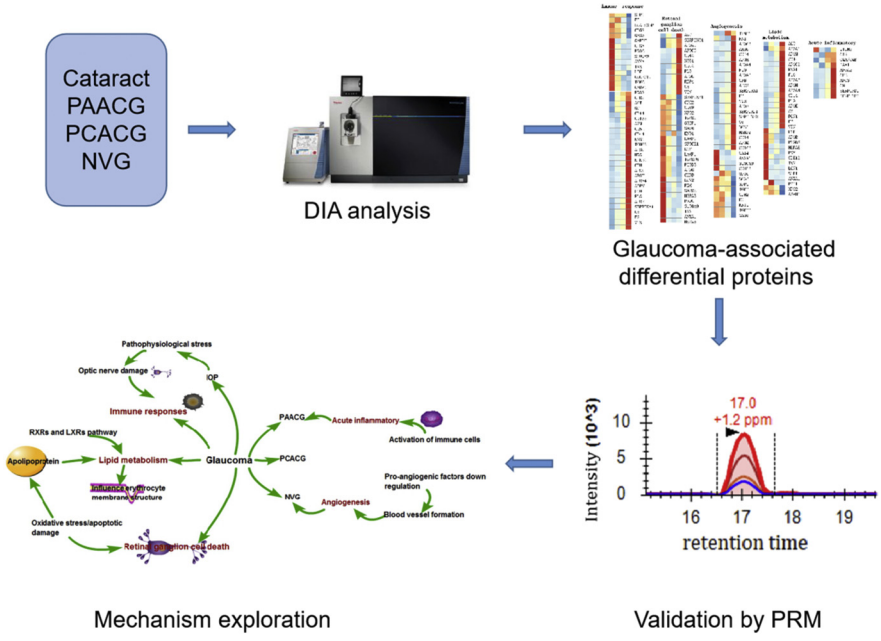

Highlights

- Aqueous humor proteome of different glaucoma (PACG, NVG) was profiled.
- Potential protein biomarkers for glaucoma were proposed.
- Potential mechanism of glaucoma was described.
- SERPIND1 was discovered to have potential value for glaucoma diagnosis.

2021, Mol Cell Proteomics *20*, 100117

https://doi.org/10.1016/j.mcpro.2021.100117

Proteome Characterization of Glaucoma Aqueous Humor

Xiaoyan Liu[1,2,‡], Xiang Liu[1,2,3,‡], Ying Wang[4,‡], Haidan Sun[1,2], Zhengguang Guo[1,2], Xiaoyue Tang[1], Jing Li[1], Xiaolian Xiao[1], Shuxin Zheng[1], Mengxi Yu[5], Chengyan He[5], Jiyu Xu[1], and Wei Sun[1,2,*]

Glaucoma is the leading cause of irreversible blindness worldwide. The proteome characterization of glaucoma is not clearly understood. A total of 175 subjects, including 57 primary acute angle-closure glaucoma (PAACG), 50 primary chronic angle-closure glaucoma (PCACG), 35 neovascular glaucoma (NVG), and 33 cataract patients, were enrolled and comparison proteomic analysis was provided. The samples were randomly divided into discovery group or validation group, whose aqueous humor proteome was analyzed by data-independent acquisition or by parallel reaction monitoring. The common proteome features of three types of glaucoma were immune response, lipid metabolism, and cell death. Three proteins, VTN, SERPIND1, and CD14, showed significant upregulation in glaucoma and could discriminate glaucoma from cataract. Mutual differential proteomic analysis of PAACG, PCACG, and NVG showed different proteome characterization of the three types of glaucoma. NVG was characterized with activated angiogenesis. PAACG was characterized with activation of inflammation response. SERPIND1 was discovered to play vital role in glaucoma occurrences, which is associated with eye transparency decrease and glucose metabolism. This study would provide insights in understanding proteome characterization of glaucoma and benefit the clinical application of AH proteome.

Glaucoma is the leading cause of irreversible blindness worldwide (1). It is a progressive optic neuropathy accompanied by retinal ganglion cell (RGC) loss, optic nerve atrophy, and visual field loss (2). An elevated intraocular pressure (IOP) is considered a hallmark of glaucoma (3). The two commonly occurring types of glaucoma are primary open-angle glaucoma (POAG) and primary angle-closure glaucoma (PACG), based on the presence of an open or closed iridocorneal angle (4). More than 50% of glaucoma-caused blindness is attributed to PACG, particularly in Asians (5). Primary acute angle-closure glaucoma (PAACG) is a type of PACG and an important cause of blindness in East Asia. PAACG occurs when the anterior chamber angle is suddenly obstructed, and the IOP rises rapidly to high levels (6). Primary chronic angle-closure glaucoma (PCACG) is caused by permanent closure of the angle due to peripheral anterior synechiae (PAS), inducing an increase in IOP. PCACG shows an increasing prevalence with age and frequently coexists with cataract (7). Besides primary glaucoma, neovascular glaucoma (NVG) is a type of secondary glaucoma, which is caused by the growth of a fibrovascular membrane secondary to a local angiogenic stimulus over the trabecular meshwork and obstructing the outflow of aqueous humor (8). NVG is most common in patients with diabetes, occlusions of major retinal vessels, carotid artery obstructive disease (9).

Glaucoma is a complex neurodegenerative ocular disease with unclear molecular mechanisms. Previous reports have focused on quantitative proteomics analysis of the AH protein profile in glaucoma (2, 3, 10–12), with multiple genetic and nongenetic risk factors. Accordingly, a high IOP is a major risk factor for glaucoma, and therapeutic pressure reduction can significantly delay disease progression [4], but the molecular mechanisms regarding how IOP leads to RGC death and optic nerve damage remain unclarified (12). Additionally, aging (13–15), genetic predispositions (16), oxidative stress (17), mitochondrial dysfunction (18), inflammatory (5, 11, 19, 20), vascular dysregulation (21), and lipid metabolism (1) have been reported to be associated with glaucoma. However, the precise etiology of glaucoma remains unclear and the molecular mechanisms of RGC loss and optic nerve atrophy remain elusive. Thus, identifying the factors that contribute to the pathogenesis and progression of this disease is crucial.

The aqueous humor (AH) directly contacts the critical site of pathogenesis in glaucoma. It serves important functions of

From the [1]Institute of Basic Medical Sciences, Chinese Academy of Medical Sciences, School of Basic Medicine, Peking Union Medical College, Beijing, China; [2]Proteomics Center, Chinese Academy of Medical Sciences, Beijing, China; [3]Application Support Center, Shanghai AB Sciex Analytical Instrument Trading Co, Ltd, Shanghai, China; [4]Department of Ophthalmology, The Second Hospital of Jilin University, Changchun, Jilin, China; [5]Clinical Laboratory, China-Japan Union Hospital of Jilin University, Changchun, Jilin, China

‡These authors contributed equally to this work.

*For correspondence: Wei Sun, sunwei1018@sina.com.

https://doi.org/10.1016/j.mcpro.2021.100117

supplying nutrients to the cornea, lens, and trabecular meshwork while maintaining refraction and the IOP of the eye (10). Therefore, it may provide insights into understanding the pathophysiology of glaucoma (12). Additionally, the discovery of proteomic biomarkers could improve our understanding of the molecular mechanisms of diseases and become a helpful diagnostic and risk-stratification tool, allowing individualized treatment for safer and more effective therapies (22). Previous reports have focused on quantitative proteomics analysis of the AH protein profile in glaucoma (2, 3, 10–12). In 2016, Kaeslin *et al.* (11) analysed the AH proteome in patients with POAG and a control group based on SWATH technology. They identified 448 proteins and found 87 proteins differentially expressed between glaucomatous and control aqueous humor. In 2018, Adav *et al.* (12) analysed the AH proteome in patients with PACG and cataract. They identified 1363 proteins and found that more than 50% were differentially expressed in PACG. An altered AH proteome in human PACG indicates oxidative stress in neuronal damage that precedes vision loss. In 2018, Kaur *et al.* (10) compared the total AH proteome of PACG, POAG, and age-related cataract eyes. They highlighted significant differences in the AH of PACG eyes compared with that of POAG and cataract eyes. The above results and differentially expressed proteins provide novel insights into understanding the disease mechanism and yielding potential prognostic biomarkers.

In this study we tried to characterize the proteome pattern of glaucoma with a large-scale sample size, and the proteome characterizations of different glaucoma were also investigated. The AH samples were recruited from 175 individual patients, including PAACG, PCACG, NVG, and age-related cataract. First, in the discovery cohort, the AH proteome characteristics of PAACG, PCACG, and NVG with cataract were compared using the DIA approach. Second, the AH proteomic features of three types of glaucoma, PAACG, PCACG, and NVG, were mutually compared. In the validation cohort, the key proteins of the above comparison were validated by PRM approach. The possible mechanisms of different glaucoma types were explored by functional annotation of differential AH proteins. This study not only provides common proteome patterns of glaucoma but also helps to understand the potential mechanism of the different types of glaucoma.

EXPERIMENTAL PROCEDURES

Experimental Design and Statistical Rationale

The purpose of this study was to measure the AH proteome of different types of glaucoma, PCACG, PAACG, and NVG to assess the potential mechanism of glaucoma. Two cohorts were enrolled as discovery cohort and validation cohort (Table 1). Glaucoma-associated proteins were firstly discovered in the discovery cohort using data-independent data acquisition (DIA) strategy and further validated in the validation cohort using parallel reaction monitoring (PRM) strategy. A mixture sample pooled from all samples was prepared as quality control (QC). QC sample was injected frequently to monitoring reproducibility of the method. Samples were randomized using random function of Microsoft Excel 2010. iRT was used as retention time reference, and MS1 data were acquired. A library was created (details described in spectral library generation) using a sample measured with data-dependent acquisition (DDA) from each experimental condition (n = 4). Principal component analysis (PCA) and heatmap virtualization were implemented using the Wukong data analysis platform (https://www.omicsolution.org/wkomics/main/). Nonparameter Wilcoxon rank-sum test was performed for significance evaluation of proteins between groups (23). The proteins that presented a fold change above 1.5 and a p-value less than 0.05 were considered differentially expressed proteins. Function and pathway were analyzed using ingenuity pathway analysis software (QIAGEN), a

TABLE 1
Demographic and clinical characteristics of the patients

Characteristics	PAACG	PCACG	NVG	Cataract
Discovery set				
Total number of eyes/cases	33/32	35/33	25/25	23/23
Age, mean (SD), year	68.4 (7.9)	61.9 (13.6)	64.12 (16.4)	69.2 (12.5)
Sex, M/F	7/26	17/18	13/12	7/16
IOP, mean (SD), mmHg	46.2 (13.1)	37.0 (12.3)	50.6 (14.2)	15.8 (2.0)
MD, median (SD)	−18.8 (7.5)	−22.7 (8.0)	-	-
VFI, mean (SD)	52.5 (29.0)	34.8 (28.1)	-	-
Subjects with hypertension or diabetes	8	15	15	5
Validation set				
Total number of eyes/cases	24/23	15/14	17/14	10/10
Age, mean (SD), year	67.8 (7.8)	63.9 (12.6)	57.1 (9.1)	73.1 (12.2)
Sex, M/F	3/21	8/7	15/2	5/5
IOP, mean (SD), mmHg	51.7 (11.2)	34.1 (10.6)	50.5 (11.9)	15.0 (2.4)
MD, median (SD)	−19.70 (8.8)	−19.9 (10.8)	-	-
VFI, mean (SD)	47.2 (35.5)	55.5 (34.5)	-	-
Subjects with hypertension or diabetes	12	8	14	2

Abbreviations: IOP, the highest intraocular pressure; MD, mean defect; NVG, neovascular glaucoma; PAACG, primary acute angle-closure glaucoma; PCACG, primary chronic angle-closure glaucoma; SD, standard deviation.

https://doi.org/10.1016/j.mcpro.2021.100117

repository of biologic interactions and functions created from millions of individually modeled relationships that range from the molecular (proteins, genes) to organism (diseases) level.

Subjects Enrollment

The study was approved by the Institutional Review Board of the Institute of Basic Medical Sciences, Chinese Academy of Medical Sciences. Informed consent was obtained from each participant before enrollment. All the subjects underwent a thorough ophthalmic evaluation, including IOP measurement, best corrected visual acuity measurement, gonioscopy testing, and fundus examination. The inclusion criteria for PAACG and PCACG were as follows: most of the angle was closed, intraocular pressure was increased, fundus changes and visual field defects were found in glaucoma optic nerve injury. The inclusion criteria for NVG were as follows: neovascularization in the angle and iris, increased intraocular pressure, and extensive ischemic changes in the retina. Patients with autoimmune diseases, malignant tumors, severe liver disease, and previous ocular surgery were excluded. The clinical parameters including age and IOP were collected for all patients and are presented in Table 1. To avoid the drug effects on AH proteome, the glaucoma patients recruited were treated with the same drug (topical alpha receptor agonists, topical carbonic anhydrase inhibitors, topical beta-blockers, and systemic carbonic anhydrase inhibitors). The studies in this work abide by the Declaration of Helsinki principles.

In total, 175 subjects, including 57 with PAACG, 50 with PCACG, 35 with NVG, and 33 with age- and gender-matched cataract as a control, were recruited for this study. The samples were divided into two sets. Set I, including 116 AH samples, was used as the discovery group and analyzed in the DIA mode. Set II, including the remaining 59 samples, was used as the validation group for PRM analysis. To evaluate the technical reproducibility of the LC-MS experiments, QC samples were generated by pooling all the samples in sets I and II in equal amounts and repeatedly analyzing them throughout the entire MS process.

Sample Preparation

AH samples were obtained from glaucoma patients during surgery. Each sample was approximately 50 to 200 μl and was aspirated from the anterior chamber using a 26-gauge needle before the start of surgery. All the samples were then immediately stored at −80 °C for further analysis.

The protein concentration of the AH samples was determined by the Bradford method. Protein digestion was carried out using the filter-aided sample preparation technique (FASP) method. For each group, a pooled sample of equal amounts of proteins from each sample was used for library generation. The proteins were denatured by incubation with 20 mM dithiothreitol at 95 °C for 5 min and then were alkylated in 55 mM iodoacetamide in the dark for 45 min. Trypsin (1:50) was added to these samples, which then were incubated at 37 °C overnight.

High-pH RPLC Separation

The pooled peptide sample of four groups was separated by high-pH RPLC columns (4.6 mm × 250 mm, C18, 3 μm; Waters), respectively. Each pooled sample was loaded onto the column in buffer A1 (H_2O, pH 10). The elution gradient was 5% to 30% buffer B1 (90% ACN, pH 10; flow rate, 1 ml/min) for 30 min. The eluted peptides were collected at one fraction per minute. After lyophilization, the 30 fractions were resuspended in 0.1% formic acid for the cataract group. For the three glaucoma groups, the 30 fractions were resuspended in 0.1% formic acid and then were concatenated into ten fractions by combining fractions 1, 11, 21, and so on.

LC-MS Analysis

The Orbitrap Fusion Lumos Tribrid (Thermo Scientific) coupled with an EASY-nLC 1000 was used for LC-MS analysis. The digested peptides were dissolved in 0.1% formic acid and separated on an RP C18 self-packing capillary LC column (75 μm × 150 mm, 3 μm). The eluted gradient was 5% to 30% buffer B2 (0.1% formic acid, 99.9% ACN; flow rate, 0.3 μl/min) for 60 min.

To generate the spectral library, the fractions from RPLC were analyzed in the DDA mode. The parameters were set as follows: the MS was recorded at 350 to 1500 m/z at a resolution of 60,000 m/z; the maximum injection time was 50 ms, the auto gain control (AGC) was 1e6, and the cycle time was 3 s. MS/MS scans were performed at a resolution of 15,000 with an isolation window of 1.6 Da and a collision energy at 32% (HCD); the AGC target was 50,000, and the maximum injection time was 30 ms.

Each sample and the QC samples were analyzed in the DIA mode. For MS acquisition, the variable isolation window DIA method with 38 windows was developed. The specific window lists were constructed based on the DDA experiment of the pooled sample. The window list of the DIA method is appended in supplemental Table S1*A*. The full scan was set at a resolution of 120,000 over the m/z range of 400 to 900, followed by DIA scans with a resolution of 30,000; the HCD collision energy was 32%, the AGC target was 1E6, and the maximal injection time was 50 ms.

Spectral Library Generation

To generate a comprehensive AH spectral library, the pooled AH sample from each group was processed. The DDA data were processed using Proteome Discoverer 2.1 (Thermo Scientific) software and searched against the human Swiss-Prot database (*Homo sapiens*, 20205 SwissProt, 2017_09 version) appended with the iRT fusion protein sequence. A maximum of two missed cleavages for trypsin was used, cysteine carbamidomethylation (+57.021 Da) was set as a fixed modification, and methionine oxidation (+15.995 Da), asparagine and glutamine deamidation (+0.984 Da), lysine carbamylation (+43.006 Da) were used as variable modifications. The parent and fragment ion mass tolerances were set to 10 ppm and 0.02 Da, respectively. The applied false discovery rate (FDR) cutoff was 0.01 at the protein level. The results were then imported to Spectronaut Pulsar (Biognosys) software to generate the library (24). Spectronaut Pulsar software allows the generation, merging, and management of spectral libraries. Next, we merged the four libraries to one AH spectral library, which contained all the information generated from the different libraries.

Data Analysis

The DIA raw data were loaded to the Spectronaut 12 to calculate peptide retention time based on iRT data. And Spectronaut provided protein identification and quantitation by matching the retention time, m/z, *etc.*, to peptide library. The retention time prediction type was set to dynamic iRT, and interference correction at the MS2 level was enabled. The MS1 and MS2 tolerance strategy was set to dynamic. It applied a correction factor to the automatically determined mass tolerance. The correction factor for ms1 and ms2 was all set as 1. The precursor posterior error probability (PEP) cutoff was set to 1. And precursors that do not satisfy the cutoff will be imputed. The top N (min: 1; max: 3) precursors per peptide were used for quantify calculation. The top N ranking order is determined by a cross-run quality measure. Peptide intensity was calculated by summing the peak areas of their respective fragment ions for MS2. Cross-run normalization was enabled to correct for systematic variance in the LC-MS performance, and a local normalization strategy was used. Normalization was based on the assumption that on average, a similar

number of peptides are up- and downregulated, and the majority of the peptides within the sample are not regulated across runs and along retention times. Protein inference, which gave rise to the protein groups, was performed on the principle of parsimony using the ID picker algorithm as implemented in Spectronaut Pulsar. All results were filtered by a Q value cutoff of 0.01 (corresponding to an FDR of 1%). Protein intensity was calculated by summing the intensity of their respective peptides. Proteins identified in more than 50% of the samples in each group were retained for further analysis. Missing values were imputed based on the k-nearest neighbour method (25). PCA was implemented using the Wu-kong data analysis platform (https://www.omicsolution.org/wkomics/main/). Nonparameter Wilcoxon rank-sum test was performed for significance evaluation of proteins between groups. The proteins that presented a fold change above 1.5 and a *p*-value less than 0.05 were considered differentially expressed proteins.

PRM Validation

Tier 3 level of the PRM analysis was developed and applied to validate the differentially expressed proteins as determined by DIA and was performed using TripleTOF 5600 (SCIEX). The separation of the peptides was performed on the RP C18 monolithic capillary LC column (50 μm × 500 mm, omics technology Co, Ltd). The eluted gradient was 5% to 30% buffer B1 (0.1% formic acid, 99.9% ACN; flow rate, 0.3 μl/min) for 60 min. For ionization, a spray voltage of 2.20 kV and a capillary temperature of 60 °C were used. The peptides were monitored using the PRM acquisition mode performing MS/MS scans of the precursor ions for all peptide markers along the complete chromatographic run. The normalized collision energy was fixed to 35%, and the accumulated time was 100 ms.

The resulting MS data were processed using Skyline (v.3.6). The peptide settings were as follows: the enzyme was set as trypsin [KR/P], the maximum missed cleavages were set as 2; the peptide length was set as 8 to 25; and the variable modifications were set as carbamidomethyl on cysteine and oxidation on methionine. The transition settings were as follows: the precursor charges were set as 2 and 3; the ion charges were set as 1 and 2; and the ion types were set as b, y. The raw data could be downloaded from iProX (https://www.iprox.cn/) with the dataset identifier IPX0002299000).

Protein Function Annotation

All the differential proteins were used for pathway analysis using Ingenuity Pathway Analysis (IPA) software (Ingenuity Systems) for network analysis. The Swissport accession numbers were uploaded to IPA software (QIAGEN). The proteins were mapped to disease and function categories and canonical pathways available in Ingenuity and other databases and were ranked by *p*-values.

RESULTS

Workflow of Aqueous Humor Proteome Analysis

In this study, 175 subjects were enrolled—116 in the discovery phase and 59 in the validation phase (Table 1). Figure 1 shows the general workflow of this study. In the discovery phase, we analyzed the proteome of AH samples from 33 PAACG, 35 PCACG, 25 NVG, and 23 cataract (control) patients using the DIA method. First, we compared the various types of glaucoma to cataract, exploring and identifying proteins differentially expressed between glaucoma and cataract. Next, we identified differential proteins among the different types of glaucoma (PAACG, PCACG, and NVG). Functional analyses of these differential proteins were used to explore the molecular mechanism of glaucoma and the further underlying mechanism of different types of glaucoma. Finally, proteins with biological significance were externally validated using an independent cohort of patients (10 with cataract, 24 with PAAGC, 15 with PCAGC, and 17 with NVG) using the PRM method.

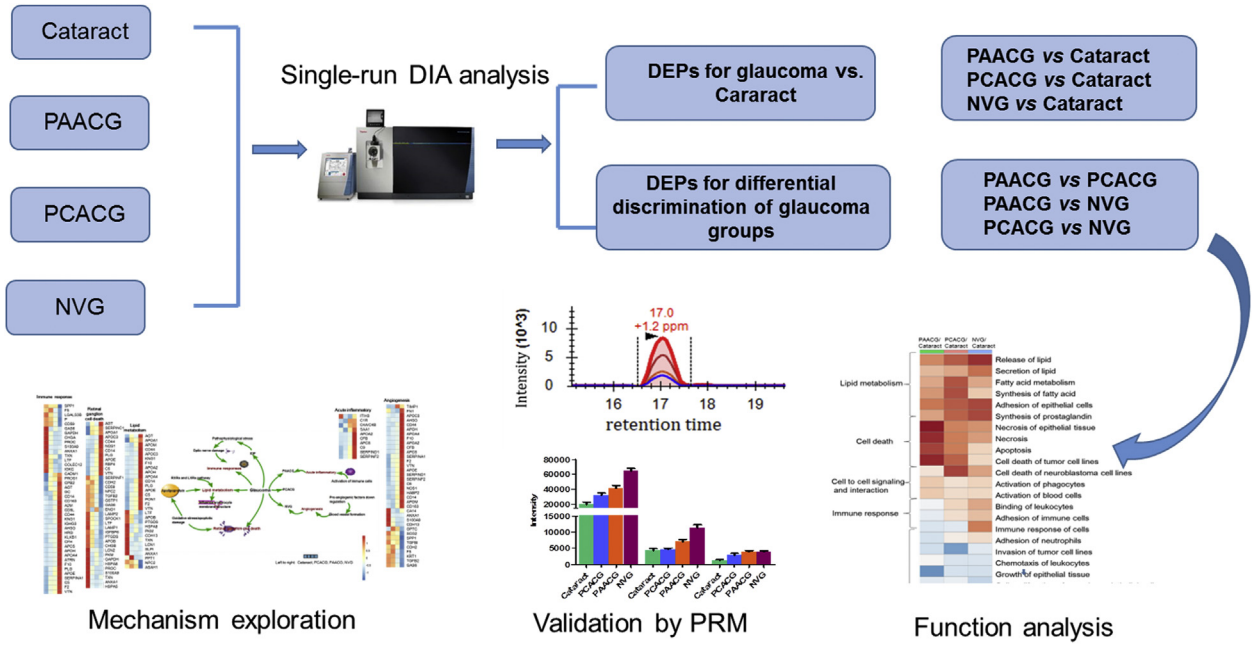

FIG. 1. **Workflow of this study**.

AH Spectral Library Generation and Protein Identification in DIA-MS

In this study, four libraries—PAACG, PCACG, NVG and cataract—were constructed by DDA 2D-LC/MS analysis. Finally, a merged library from the above four libraries was constructed by pulsar, and 12,661 precursors, 9272 peptides, and 887 protein groups were obtained from the merged AH spectral library (supplemental Table S1, *B–G,* Supplemental Data 1). Number of proteins in PCACG and NVG library was less than that in PAACG library, which might be associated the characteristics of glaucoma. The detailed possible reason needs further exploration (1). For DIA analysis, 636 AH proteins were detected with a protein FDR <1%. For each sample, 520 protein groups were identified by peptide-spectrum matching. In total, 490 protein groups with quantitative data in more than 50% of samples in each group were selected for further analysis (supplemental Table S2*A*).

DIA and PRM Data Quality Control

Technical repeatability was evaluated by calculating the CV of the protein abundances among the 27 QC replicates. The median and 90% quantile of technical CVs were 0.17 and 0.52, respectively. Pearson's correlation coefficients were approximately 1 among 27 QC replicates (supplemental Fig. S1*A*) and showed good technical reproducibility.

For PRM analysis, 423 peptides of 231 DEPs were quantified (supplemental Table S2*B*). The median and 90% quantile of the technical CVs were 0.22 and 0.40, respectively. Pearson's correlation coefficients were approximately 1 among 26 QC replicates (supplemental Fig. S1*A*), indicating good technical reproducibility.

For biological replicates reliability evaluation, we applied Hoteling's T2 analysis.

T2 range is basically calculated as the sum over the selected range of components of the scores in square divided by their standard deviations in square. Hence, T2 range is the distance in the model plane (score space) from the origin, in the specified range of components. In present study, biological replicates in each group were within the 99% confidence limit (supplemental Fig. S1*B*).

Differential Proteomic Analysis Between Glaucoma and Cataract

Differential Proteomic Analysis—AH proteome differences between glaucoma and cataract were first analyzed by the unbiased statistical method PCA. Apparent separation trends could be observed between glaucoma and cataract. The separation of NVG and cataract was the most obvious. Additionally, some overlay between PCACG and cataract was observed, indicating less separation of the groups (Fig. 2*A*, supplemental Fig. S2, *A–C*). Next, the differentially expressed proteins in glaucoma compared with cataract were defined using the criterion of a fold change greater than 1.5 and B-H adjusted *p* value less than 0.05 (supplemental Fig. S2, *D–F*). Thus, the numbers of differentially expressed proteins in PAACG, PCACG, and NVG compared with cataract were 182, 111, and 262 proteins, respectively (supplemental Table S3*A*). Differential proteins with higher levels in the glaucoma groups included apolipoproteins (APOA1, APOA2, APOA4, APOE, APOH), complement proteins (C1R, C2, C4A/C4B, C5, C6, C8A, C9, CFB, CFI) , and inflammatory protein (SERPINA1, SERPINF2, CD14, GC, ITIH4). By contrast, proteins with lower expression levels included IGFBP4, IGFBP6, TGFB2, and ANXA1, which were mainly involved in cellular movement and development.

Functional Annotation of Differential Proteins—The differentially expressed proteins of glaucoma and cataract were submitted to the canonical pathway and function analysis using IPA. The top canonical pathways associated with immune and inflammatory regulation (*e.g.*, LXR/RXR activation, acute phase response signaling, and the complement system) were upregulated in PAACG, PCACG, and NVG. By contrast, the coagulation system and intrinsic prothrombin activation pathway were downregulated in the three glaucoma groups relative to the cataract group (supplemental Table S3, *B–D*). Disease and function analyses showed that the functions of lipid metabolism, cell death, cell-to-cell signaling and interaction, and immune response were activated in glaucoma. Additionally, cellular movement and development were deactivated in glaucoma (Fig. 2*B*).

PRM Validation—To confirm the results obtained by DIA analysis, DEPs with biological significance were further validated by the PRM method using an independent batch of patients. The differential proteins showing significant differences in group comparison, and with the same change trend with these detected using the DIA method, were selected. After screening the spectra library of the AH proteome and filtering the peptides according to previous criteria (26), 26, 15, and 78 DEPs were validated in PAACG *versus* cataract, PCACG *versus* cataract, and NVG *versus* cataract, respectively (supplemental Table S3*E*).

AUC Evaluation—We further evaluated the accuracy of the DEPs to discriminate PAACG, PCACG, and NVG from cataract. The combination of AH proteins with the highest AUC values is shown in supplemental Fig. S3. The ROC areas of the three comparisons were all above 0.90. Additionally, the sensitivity and specificity were above 80% (supplemental Table S3*F*).

Common DEPs of the three comparisons reflect common features of these three types of glaucoma. Three proteins, VTN, SERPIND1, and CD14, were common DEPs in three types of glaucoma relative to cataract. The three DEPs showed the highest expression level in NVG, followed by PAACG, and showed the lowest levels in PCACG (Fig. 2*C* and Table 2). The combination of the three DEPs could separate glaucoma from cataract with an AUC value of 0.88 for the discovery group and 0.85 for the validation group (Fig. 2*D* and supplemental Table S3*G*).

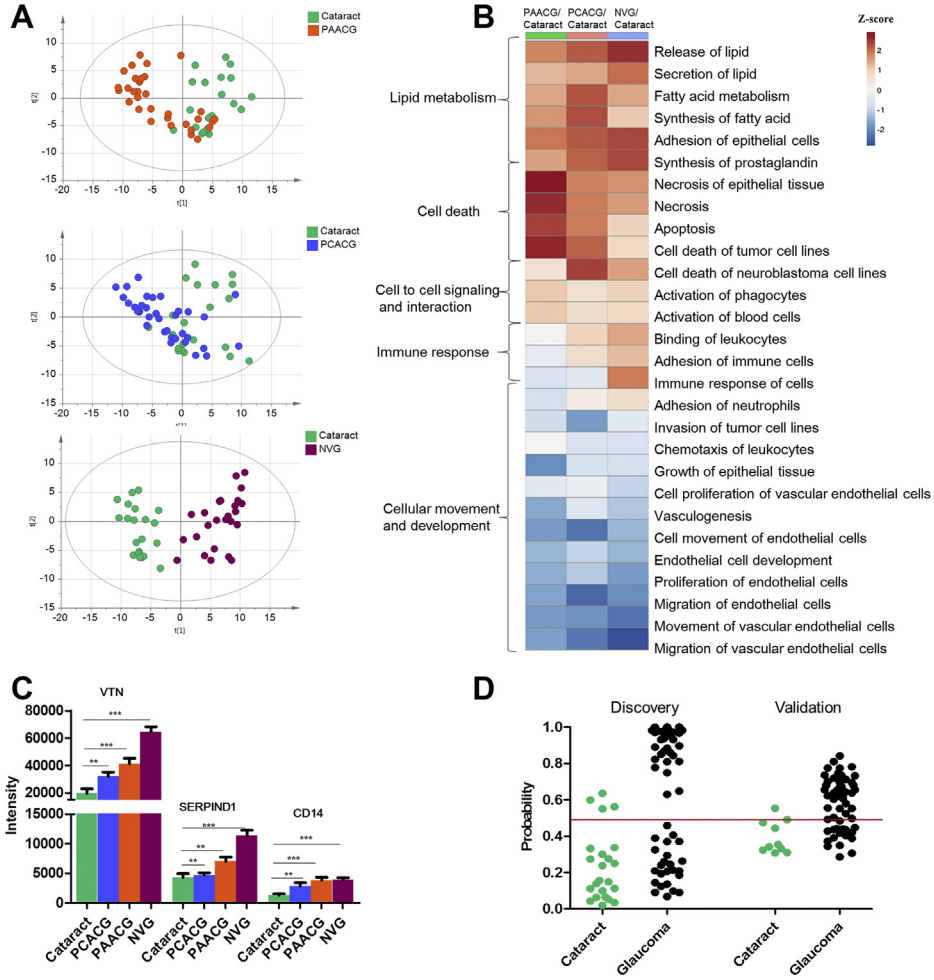

FIG. 2. **Comparison of the AH proteomics of glaucoma and cataract.** *A*, PCA plots of three types of glaucoma compared with cataract by DIA analysis (discovery group). *B*, comparison of disease and function analyses of differential proteins between glaucoma and cataract. The value represents the z score calculated to predict the status of function. The Z score with a positive value indicates activation, and a negative value indicates inhibition. *C*, relative intensity of VTNC, SERPIND1, and CD14 proteins in the glaucoma and cataract groups by PRM analysis (validation group). Nonparameter Wilcoxon rank-sum test was performed for significance evaluation of proteins. $^{*}p < 0.05$; $^{**}p < 0.01$; $^{***}p < 0.001$. *D*, discrimination accuracy for the separation of glaucoma and cataract using the proteins VTNC, SERPIND1, and CD14 in the discovery set (DIA, *left graph*) and validation data sets (PRM, *right graph*).

Differential Proteomic Analysis Among the Three Types of Glaucoma

Differential Proteomic Analysis—Compared with the cataract group, the three glaucoma groups showed similar molecular features, increased lipid metabolism, cell death, and immune response and decreased cellular movement and development (Fig. 2*B*). Additionally, we further focused on the different proteome characteristics of NVG, PAACG, and PCACG to understand the underlying disease mechanism of different types of glaucoma.

PCA and PLS-DA plots of the three glaucoma groups showed separation to some extent (supplemental Fig. S4 and Fig. 3*A*). The NVG and PCACG groups showed obvious separation and PAACG overlays with the other two groups. Next, differential proteins were selected with the criterion of a fold change greater than 1.5 and B-H adjusted *p* less than 0.05. Thus, 97, 218, and 222 differential proteins in PAACG *versus* PCACG, PAACG *versus* NVG, and PCACG *versus* NVG were identified, respectively (supplemental Table S4*A*).

Functional Annotation of Differential Proteins—To explore the molecular mechanisms and biological processes that are altered in different types of glaucoma, we performed IPA analyses on differential proteins of the three comparisons. The top disturbed pathways were LXR/RXR activation, FXR/RXR activation, complement system, acute phase response signaling, and prothrombin activation pathway, with a similar pattern in the three comparisons. Comparison of disease and function analyses showed that the functions of cardiovascular system development, cell-to-cell signaling and interaction, cellular movement, inflammatory response, lipid metabolism,

TABLE 2
Common differentially expressed proteins in the glaucoma and cataract groups

A. Three common differentially expressed proteins in the glaucoma groups relative to cataract

Group	Strategy	Significance	P04004	P05546	P08571
PAACG/Cataract	DIA	FC	2.66	2.41	3.42
		p value	5.42E-06	4.92E-05	7.42E-04
	PRM	FC	2.56	1.69	2.95
		p value	2.12E-04	3.18E-02	9.29E-05
PCACG/Cataract	DIA	FC	2.07	2.03	1.91
		p value	3.16E-05	7.52E-05	3.45E-03
	PRM	FC	1.8	1.57	1.64
		p value	1.39E-02	2.69E-03	2.24E-02
NVG/Cataract	DIA	FC	5.37	6.34	9.52
		p value	2.03E-08	4.34E-05	3.32E-09
	PRM	FC	3.84	2.55	3.36
		p value	3.93E-09	1.70E-06	5.46E-06

B. Three common differentially expressed proteins among the three types of glaucoma

Group			P05546	Q16568	Q96JP9
PAACG/PCACCG	DIA	FC	1.29	0.1	0.33
		p value	3.59E-02	1.54E-03	1.72E-02
	PRM	FC	1.5	0.48	0.62
		p value	8.72E-03	1.41E-02	2.14E-02
NVG/PAACG	DIA	FC	2.43	0.09	0.9
		p value	7.16E-03	3.39E-02	2.57E-02
	PRM	FC	1.62	0.32	0.57
		p value	6.93E-04	5.15E-05	1.37E-02
NVG/PCACG	DIA	FC	3.12	0.008	0.3
		p value	4.97E-04	8.35E-06	3.99E-04
	PRM	FC	2.42	0.15	0.35
		p value	1.71E-06	3.38E-04	4.75E-04

organismal injury and abnormalities, and cell death and survival were dysregulated in the different types of glaucoma. Compared with the PCACG and PAACG groups, the NVG group showed higher activation of the above functions. Additionally, PAACG showed higher activation of these functions than PCACG (supplemental Table S4, *B–D*). These comparisons indicated the function dysregulation degree of the three glaucoma types (Fig. 3*B*).

PRM Validation—Further PRM analysis was performed to confirm the results obtained by DIA analysis using an independent cohort of patients. The differential proteins showing significant differences in group comparison, and with the same change trend with these detected using the DIA method, were selected. After screening the spectra library of the AH proteome and filtering the peptides, 25, 31, and 91 proteins were verified that showed significant differences and the same trends as DIA analysis (supplemental Table S4*E*).

AUC Evaluation—We further evaluated the accuracy of the DEPs to discriminate PAACG, PCACG, and NVG. The combination of AH proteins with the highest AUC values is shown in supplemental Fig. S5. The ROC areas for the three comparisons were all close to 1 in the validation group. Additionally, the sensitivity and specificity were above 80% (supplemental Table S4*F*).

Three proteins, SERPIND1, CARTPT, and CDHR1, were identified and confirmed to be expressed differently among the three group comparisons (Table 2; Fig. 3*C*). The combination of the three proteins could discriminate the different types of glaucoma with AUC values of 0.74, 0.85, and 1 for PAACG *versus* PCACG, PAACG *versus* NVG, and PCACG *versus* NVG in the validation group, respectively (Fig. 3*D* and supplemental Table S4*G*).

SERPIND1, also known as heparin cofactor II, is not only expressed differently between the cataract control and glaucoma groups but also shows significantly different levels among the glaucoma subtypes. These results suggest that SERPIND1 has potential value for glaucoma diagnosis and differential diagnosis.

DISCUSSIONS

In this study, we compared glaucoma to cataract and mutually compared the different types of glaucoma. The AH proteomic results suggest that activated immune response, lipid metabolism, and cell death in glaucoma were related to glaucoma. Our data shed light on the proteome changes reflected in glaucoma AH, which could potentially help to understand the underlying molecular mechanism of different

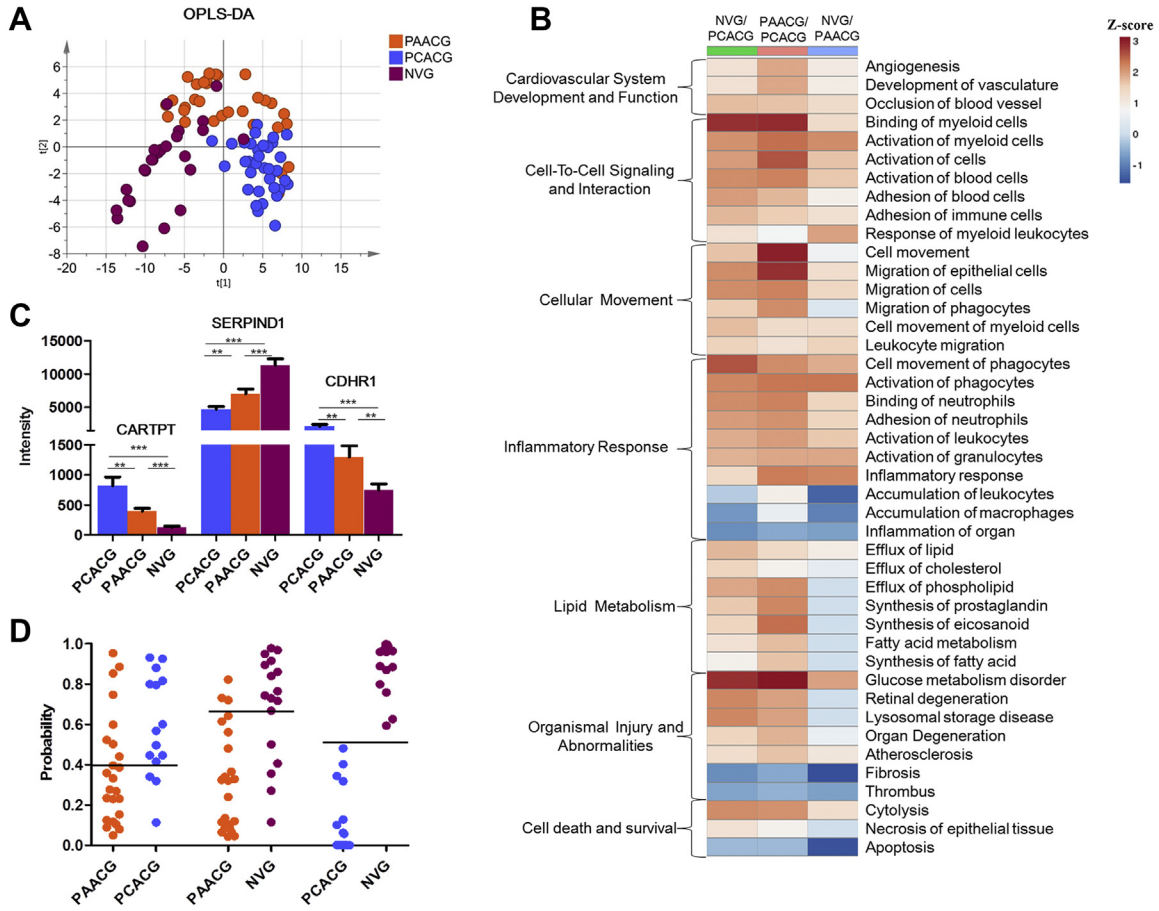

FIG. 3. **Comparison of the AH proteomics of PAACG, PCACG, and NVG.** *A*, PLS-DA score plot for the virtualization of PAACG, PCACG, and NVG separation in the discovery group (DIA data). *B*, comparison of disease and function analyses of differentially expressed proteins among the three types of glaucoma. The value represents the z score calculated to predict the status of function. A Z score with a positive value indicates activation, and a negative value indicates inhibition. *C*, relative intensity of SERPIND1, CART, and CDHR1 in the PAACG, PCACG, NVG, and cataract groups by PRM analysis. *D*, discrimination accuracy of PAACG, PCACG, and NVG using the three common differentially expressed proteins in "*C*" in the validation group (PRM data).

types of glaucoma and expand approaches for glaucoma diagnosis and differential diagnosis.

AH Proteomic Characterization of Glaucoma

By comparing the AH proteome in glaucoma and cataract, we found several disturbed pathways in glaucoma, including lipid metabolism, immune response, and cell death function. These pathways and functions showed an activated status in glaucoma, giving insights into glaucoma mechanism.

Lipid Metabolism in Glaucoma—Lipid metabolism was found to be activated in glaucoma relative to cataract. Several researchers have discovered lipid metabolism disturbance in POAG (1, 27). However, no study has explored lipid metabolism change in PCAG to our knowledge. The lipid metabolism activation-induced higher lipid content is an important cause of the unstable IOP in glaucoma (28). Additionally, lipid metabolism disturbance could influence erythrocyte membrane structure, further disturbing the material exchange of microcirculation and optic disc capillary (28). The molecular mechanism of lipid metabolism activation in glaucoma might be complex, and we discuss the potential molecular mechanism as follows.

The activated immune response and RXR and LXR pathway have been reported to contribute to lipid metabolism disturbance in open-angle glaucoma (1). RXR and LXR activation is the top disturbed pathway discovered in the present study. Previous studies on glaucoma have reported that the RXR gene interacts with the upstream regulator LXR to regulate lipid metabolism, inflammation, and macrophage activation (29). Additionally, our study found increased expression levels of apolipoproteins (APOE, APOH APOA1, APOA2, APOA4) in glaucoma, probably resulting from oxidative stress and apoptotic damage (30). Apolipoproteins play central roles in lipid metabolism. They are involved in the transport and redistribution of lipids among various cells and tissues, through their role as cofactors for enzymes of lipid metabolism (31). Increased levels of apolipoproteins might regulate lipid metabolism and homeostasis in glaucoma patients (32) (Fig. 4).

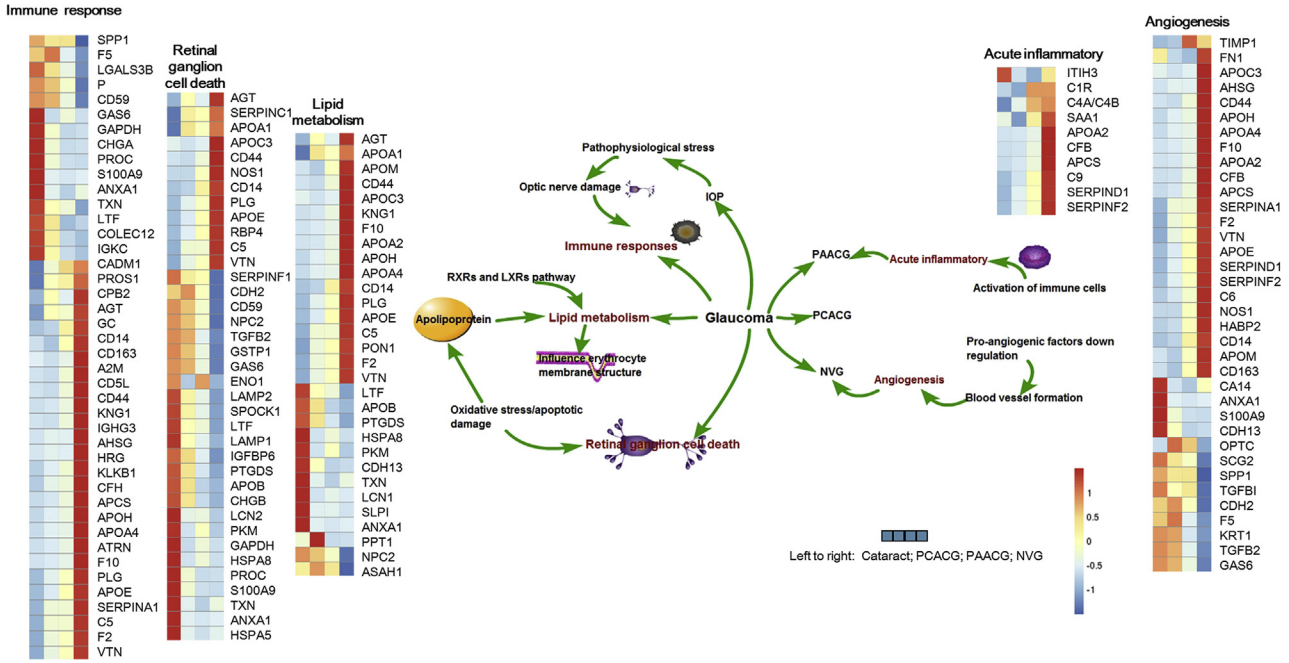

FIG. 4. **Key pathway, function, and proteins characterized in PAACG, PCACG, and NVG patients.** Immune response, lipid metabolism, and cell death were activated in glaucoma patients. PAACG is associated with an acute inflammatory condition, and NVG is associated with angiogenesis (47, 51).

Immune Response in Glaucoma—Previous studies have reported that elevated IOP could cause pathophysiological stress, further damaging the optic nerve and subsequently triggering secondary immune or autoimmune responses (5, 33). Studies have shown that high IOP is the direct cause of the immune response in early glaucoma (34). T-cell immune dysfunction caused by high intraocular pressure is an important factor of glaucomatous neurodegeneration (33). In this study, immune-response-related proteins (*e.g.*, SERPINF2, CD14, GC, ITIH4, SERPIND1) and complement proteins (*e.g.*, C1R, C2, C4A/C4B, C5, C6, C8A, C9, CFB, and CFI) showed higher expression levels in glaucoma compared with cataract. Most of these proteins were reported to regulate inflammatory function and to be upregulated in AH proteomics in POAG (1, 2, 35). CD14, a pattern recognition receptor, could enhance innate immune responses to infection by sensitizing host cells to bacterial lipopolysaccharide, lipoproteins, lipoteichoic acid, and other acylated microbial products (36). Higher expression of CD14 in glaucoma perhaps activates TLR4/MD2/CD14 receptor complex formation and induces the release of inflammatory cytokines (37), such as ITIH4, TIMP1, F2, and APOA1/2, which were discovered to show a higher expression level in glaucoma relative to cataract in this study (Fig. 4). VTN was a significantly upregulated common protein in three glaucoma subtypes. VTN, a prominent inflammatory regulatory glycoprotein and adhesion molecule, had been detected to be upregulated in vitreous humor in retinal vein occlusion (38). It was involved in complement regulation, T-cell cytolysis, and cellular adhesion. Its functions are dependent on its binding to various matrix and cellular components (39), which in turn stabilizes or activates a variety of biological macromolecules. One of the multiple functions of VTN is to act as a regulator of the complement system. The complement system is a powerful effector mechanism in inflammatory response, during which VTN acts as an important regulator (38). The present demonstration of increased levels of VTN supports the notion that the increment in vitronectin activates the complement cascade, promoting inflammatory response during glaucoma occurence.

Increased Cell Death in Glaucoma—Cell death was increased in the glaucoma groups relative to the cataract group. A crucial element in the pathophysiology of all forms of glaucoma is the death of RGCs. The mechanism is complex and involves various molecular signals—acting alone or in cooperation to promote RGC death—such as axonal transport failure, toxic proneurotrophins, activation of intrinsic and extrinsic apoptotic signals, mitochondrial dysfunction, and oxidative stress (40). In this study, 17 proteins associated with cell death showed significant differences between glaucoma and cataract, such as HSPs, CAT, and TXN. CAT and TXN, factors that protect cells from the toxic effects of hydrogen peroxide, were downregulated in glaucoma. Oxidative-stress-induced damage could subsequently contribute to cell death in glaucoma patients (41). Additionally, TXN could inhibit caspase-3 activity by nitrosylating the active-site Cys of CASP3 in response to nitric oxide (42). Low expression of TXN

probably promotes cell apoptosis in glaucoma through CASP3 regulation (Fig. 4).

Cataract patients were enrolled as controls of glaucoma. Since incidence rate of hypertension in cataract is much lower than that in glaucoma (43), the number of hypertension cases in cataract is less than that in glaucoma. Differential proteins between glaucoma and cataract might be partly due to hypertension effect. Therefore, the specific biomarkers of glaucoma need more validation in the future. Additionally, the glaucoma patients enrolled in present study were all treated with same drugs, while cataract patients were not treated with any drugs. The observed different protein expressions between glaucoma and cataract were partly due to drug effect.

Molecular Mechanism of Different Type of Glaucoma

AH proteome mutual comparison analysis showed significantly different proteome characterisation of these three types of glaucoma. PCACG showed less function disturbance. Clinically, PCACG inflammation is not generally observed, although residual inflammation may have been present from prior iridotomies, no obvious inflammatory reaction was observed in the aqueous humor of PCACG (44). Moreover, elevated IOP in PCACG was suggested to be associated with increased levels of cytokines; therefore, it is a potential stimulus for their production (45).

Neovascular glaucoma is a kind of secondary glaucoma, often secondary to retinal vein occlusion, diabetic retinopathy (DR), ocular ischemic syndrome, and central retinal artery obstruction (8). VTN, APOA4, CD14, and CFB, as biomarkers of retinal inflammation in patients with DR (46), were highly expressed in the AH of NVG patients in our studies. Except for inflammation-related proteins, 35 differential proteins in NVG were associated with neovascularization. Neovascularization is a multistep process that involves complex interactions of various angiogenic actors. New vessel formation in the eye is affected to a large extent by an imbalance among proangiogenic factors, such as antiangiogenic factors (*e.g.*, pigment epithelium-derived factor) (47). Pigment epithelium-derived factor, also known as SERPINF1, is downregulated in NVG and is an antiangiogenic factor that inhibits blood vessel formation (48). SERPIND1, which shows the highest level in NVG, is likely an angiogenesis factor. SERPIND1 promotes angiogenesis *via* the upregulation of endothelial cell movement and the AMP-activated protein kinase–endothelial nitric-oxide synthase signaling pathway (49). Additionally, in NVG patients, glucose metabolism disorder is marked by downregulated glycolytic enzymes involved in the glycolysis and gluconeogenesis pathways and carbon metabolism. These results suggest that energy metabolism reduction (disorder) in NVG likely counters oxidative stress through tissue repair or the removal of damaged tissues that also requires energy costs (50).

Compared with PCACG, PAACG showed activation of inflammation response, cellular movement, and cell-to-cell signaling interaction, marked with activation of leukocytes, neutrophils, myeloid cells, and phagocytes. These results indicated a more severe immune response in PAAGC, a finding that corresponds with clinical symptoms that PAAGC shows an early “acute inflammatory” condition (51). Inflammatory-related molecules, including APCS, C4A, CD14, CD44, GRN, and SAA1, were found to be upregulated in PAACG relative to PCACG. C4A is a protein of the complement system, which is another defence system besides innate immune cells. The activated complement system clears cell and tissue debris. There is accumulating knowledge that complement disorder is responsible for numerous immune-mediated and inflammatory disorders, including glaucoma (52). C4A has been reported to be associated with activation of the acute phase response (53), which occurs during PAACG occurrence.

SERPIND1, a Vital Protein in Glaucoma

SERPIND1, also known as heparin cofactor II, was expressed at significantly higher levels in PAACG, PCACG, and NVG, relative to cataract. Additionally, SERPIND1 showed significant differences in differential comparisons of PAACG, PCACG, and NVG. The above results indicate the vital function of SERPIND1 in glaucoma.

SERPIND1 is a serine protease inhibitor (serpin) involved in the negative regulation of endopeptidase activity. It could further influence the transparency of ocular tissues (54), which is a common symptom in these three types of glaucoma. Additionally, SERPIND1 has the function of inactivating thrombin action, which is associated with glucose metabolism. Higher expression of SERPIND1 in glaucoma could probably regulate glucose homeostasis in a beneficial direction (55). The highest level of SERPIND1 is likely the response to glucose disorder, especially in the NVG group accompanied by diabetes. Glucose is essential for the first step of energy metabolism, glycolysis. During low oxygen availability, lactate is formed from glucose. It is tempting to suggest that glaucomatous neurodegeneration may be correlated with lactate homeostasis (56). Recent studies suggest a neuroprotective role of lactate in the retina (57). Additionally, lactate is the preferred energy source for most abundant retinal glial cells, Müller cells (56). Furthermore, SERPIND1 plays an important role in the angiogenesis process, especially in NVG patients, as discussed above.

In present study, pathways of immune response and lipid metabolism showed activated in glaucoma, which could act as potential intervention target in clinic. For example, in clinical work, clinicians have used topical steroids to reduce anterior chamber inflammation and immune response in glaucoma patients (58). Additionally, lipid-related interventions could have potential value for glaucoma treatment. Glaucoma-related proteins could act as drug targets. Thus, we screened these differential proteins with clinical targeted drugs as shown in supplemental Table S3*A*. Overall 39 differential proteins have targeted drugs in clinic, which have potential value for glaucoma intervention. For example,

complement C5 showed significantly upregulated in glaucoma. The monoclonal antibody against complement factor C5 could prevent optic nerve damage in glaucoma model. Therefore, complement inhibition could serve as a new therapeutic tool for glaucoma (59). Up to date, there have no diagnostic biomarkers in clinic. In present study, we tried to discover potential biomarkers for glaucoma. Protein panels were proposed to show high diagnosis accuracy for glaucoma, including TIMP1, CD14 for PAACG, APOA1, VTN, and ANXA1 for PCACG, VTN for NVG. These proteins have potential value for glaucoma diagnosis.

CONCLUSION

Our work explored the differential proteome of glaucoma and cataract. Three types of glaucoma, PAACG, PCACG, and NVG, were individually analyzed to investigate common features relative to cataract and different features among the three types of glaucoma. Our results suggest that lipid metabolism, immune response, and cell death were significantly activated in glaucoma relative to cataract, and these functions showed different disorder degree among the three types of glaucoma. This study demonstrated that the AH proteome could reflect the characteristics of glaucoma. This might help to understand the glaucoma mechanism, diagnose disease much better in the future, and identify novel treatments.

DATA AVAILABILITY

The raw data could be downloaded from iProX (integrated Proteome resources) with the dataset identifier IPX0002299000 or the corresponding ProteomeXchange ID PXD027686.

Supplemental data—This article contains supplemental data.

Acknowledgments—This work was supported by the National Key Research and Development Program of China (No. 2016 YFC 1306300, 2018YFC0910202), National Natural Science Foundation of China (No. 30970650, 31200614, 31400669, 81371515, 81170665, 81560121, 81572082), Beijing Natural Science Foundation (No. 7173264, 7172076), Peking Union Medical College Hospital (No. 2016-2.27), and Biologic Medicine Information Center of China, National Scientific Data Sharing Platform for Population and Health. The funding bodies played no role in the design of the study and collection, analysis, and interpretation of data and in writing the manuscript.

Author contributions—Xiaoyan Liu and Xiang Liu writing-original draft; Xiaoyan Liu, Xiang Liu, W. S., W. Y., J. X., C. H., and M. Y. data curation; W. S. and W. Y. conceptualization; W. S. and W. Y. methodology; W. S. and W. Y. writing-review and editing; J. X., X. X., S. Z., X. T., and J. L. investigation; Z. G. and H. S. formal analysis.

Conflict of interest—All authors have no conflict of interest

Abbreviations—The abbreviations used are: AH, aqueous humor; DDA, data-dependent acquisition; DIA, data-independent data acquisition; DR, diabetic retinopathy; FASP, filter-aided sample preparation; FDR, false discovery rate; IOP, intraocular pressure; IPA, Ingenuity Pathway Analysis; NVG, neovascular glaucoma; PACG, primary angle-closure glaucoma; PAS, peripheral anterior synechiae; PCA, principal component analysis; PCACG, primary chronic angle-closure glaucoma; PEP, posterior error probability; POAG, primary open-angle glaucoma; PPACG, primary acute angle-closure glaucoma; PRM, parallel reaction monitoring; QC, quality control; RGC, retinal ganglion cell.

Received December 30, 2020, and in revised from, May 17, 2021
Published, MCPRO Papers in Press, June 30, 2021, https://doi.org/10.1016/j.mcpro.2021.100117

REFERENCES

1. Sharma, S., Bollinger, K. E., Kodeboyina, S. K., Zhi, W., Patton, J., Bai, S., Edwards, B., Ulrich, L., Bogorad, D., and Sharma, A. (2018) Proteomic alterations in aqueous humor from patients with primary open angle glaucoma. *Invest. Ophthalmol. Vis. Sci.* **59**, 2635–2643
2. Kliuchnikova, A. A., Samokhina, N. I., Ilina, I. Y., Karpov, D. S., Pyatnitskiy, M. A., Kuznetsova, K. G., Toropygin, I. Y., Kochergin, S. A., Alekseev, I. B., Zgoda, V. G., Archakov, A. I., and Moshkovskii, S. A. (2016) Human aqueous humor proteome in cataract, glaucoma, and pseudoexfoliation syndrome. *Proteomics* **16**, 1938–1946
3. Adav, S. S., Wei, J., Terence, Y., Ang, B. C. H., Yip, L. W. L., and Sze, S. K. (2018) Proteomic analysis of aqueous humor from primary open angle glaucoma patients on drug treatment revealed altered complement activation cascade. *J. Proteome Res.* **17**, 2499–2510
4. Shree, S. N., George, R., Shantha, B., Lingam, V., Vidya, W., Panday, M., Sulochana, K. N., and Coral, K. (2019) Detection of proteins associated with extracellular matrix regulation in the aqueous humour of patients with primary glaucoma. *Curr. Eye Res.* **44**, 1018–1025
5. Zhang, J. L., Song, X. Y., Chen, Y. Y., Nguyen, T. H. A., Zhang, J. Y., Bao, S. S., and Zhang, Y. Y. (2019) Novel inflammatory cytokines (IL-36, 37, 38) in the aqueous humor from patients with chronic primary angle closure glaucoma. *Int. Immunopharmacol.* **71**, 164–168
6. Zhang, X., Liu, Y., Wang, W., Chen, S., Li, F., Huang, W., Aung, T., and Wang, N. (2017) Why does acute primary angle closure happen? Potential risk factors for acute primary angle closure. *Surv. Ophthalmol.* **62**, 635–647
7. Lee, C. K., Rho, S. S., Sung, G. J., Kim, N. R., Yang, J. Y., Lee, N. E., Hong, S., and Kim, C. Y. (2015) Effect of goniosynechialysis during phacoemulsification on IOP in patients with medically well-controlled chronic angle-closure glaucoma. *J. Glaucoma* **24**, 405–409
8. Havens, S. J., and Gulati, V. (2016) Neovascular glaucoma. *Dev. Ophthalmol.* **55**, 196–204
9. Quigley, H. A. (2011) Glaucoma. *Lancet* **377**, 1367–1377
10. Kaur, I., Kaur, J., Sooraj, K., Goswami, S., Saxena, R., Chauhan, V. S., and Sihota, R. (2019) Comparative evaluation of the aqueous humor proteome of primary angle closure and primary open angle glaucomas and age-related cataract eyes. *Int. Ophthalmol.* **39**, 69–104
11. Kaeslin, M. A., Killer, H. E., Fuhrer, C. A., Zeleny, N., Huber, A. R., and Neutzner, A. (2016) Changes to the aqueous humor proteome during glaucoma. *PLoS One* **11**, e0165314
12. Adav, S. S., Wei, J., Qian, J., Gan, N. Y., Yip, L. W. L., and Sze, S. K. (2019) Aqueous humor protein dysregulation in primary angle-closure glaucoma. *Int. Ophthalmol.* **39**, 861–871
13. Guedes, G., Tsai, J. C., and Loewen, N. A. (2011) Glaucoma and aging. *Curr. Aging Sci.* **4**, 110–117

14. Ashworth Briggs, E. L., Toh, T., Eri, R., Hewitt, A. W., and Cook, A. L. (2018) Uteroglobin and FLRG concentrations in aqueous humor are associated with age in primary open angle glaucoma patients. *BMC Ophthalmol.* **18**, 57
15. Mirzaei, M., Gupta, V. B., Chick, J. M., Greco, T. M., Wu, Y., Chitranshi, N., Wall, R. V., Hone, E., Deng, L., Dheer, Y., Abbasi, M., Rezaeian, M., Braidy, N., You, Y., Salekdeh, G. H., *et al*. (2017) Age-related neurodegenerative disease associated pathways identified in retinal and vitreous proteome from human glaucoma eyes. *Sci. Rep.* **7**, 12685
16. Whitmore, A. V., Libby, R. T., and John, S. W. (2005) Glaucoma: Thinking in new ways-a role for autonomous axonal self-destruction and other compartmentalised processes? *Prog. Retin. Eye Res.* **24**, 639–662
17. Izzotti, A., Bagnis, A., and Sacca, S. C. (2006) The role of oxidative stress in glaucoma. *Mutat. Res.* **612**, 105–114
18. Kamel, K., Farrell, M., and O'Brien, C. (2017) Mitochondrial dysfunction in ocular disease: Focus on glaucoma. *Mitochondrion* **35**, 44–53
19. Liu, Z., Fu, G., and Liu, A. (2017) The relationship between inflammatory mediator expression in the aqueous humor and secondary glaucoma incidence after silicone oil tamponade. *Exp. Ther. Med.* **14**, 5833–5836
20. Kokubun, T., Tsuda, S., Kunikata, H., Yasuda, M., Himori, N., Kunimatsu-Sanuki, S., Maruyama, K., and Nakazawa, T. (2018) Characteristic profiles of inflammatory cytokines in the aqueous humor of glaucomatous eyes. *Ocul. Immunol. Inflamm.* **26**, 1177–1188
21. Grieshaber, M. C., Mozaffarieh, M., and Flammer, J. (2007) What is the link between vascular dysregulation and glaucoma? *Surv. Ophthalmol.* **52 Suppl 2**, S144–S154
22. Velez, G., Tang, P. H., Cabral, T., Cho, G. Y., Machlab, D. A., Tsang, S. H., Bassuk, A. G., and Mahajan, V. B. (2018) Personalized proteomics for precision health: Identifying biomarkers of vitreoretinal disease. *Transl. Vis. Sci. Technol.* **7**, 12
23. Shainker, S. A., Silver, R. M., Modest, A. M., Hacker, M. R., Hecht, J. L., Salahuddin, S., Dillon, S. T., Ciampa, E. J., D'Alton, M. E., Otu, H. H., Abuhamad, A. Z., Einerson, B. D., Branch, D. W., Wylie, B. J., Libermann, T. A., *et al*. (2020) Placenta accreta spectrum: Biomarker discovery using plasma proteomics. *Am. J. Obstet. Gynecol.* **223**, 433.e1–433.e14
24. Zhao, M., Liu, X., Sun, H., Guo, Z., Liu, X., and Sun, W. (2019) Evaluation of urinary proteome library generation methods on data-independent acquisition MS analysis and its application in normal urinary proteome analysis. *Proteomics Clin. Appl.* **13**, e1800152
25. Afshinnia, F., Rajendiran, T. M., Wernisch, S., Soni, T., Jadoon, A., Karnovsky, A., Michailidis, G., and Pennathur, S. (2018) Lipidomics and biomarker discovery in kidney disease. *Semin. Nephrol.* **38**, 127–141
26. Sun, H., Wang, D., Liu, D., Guo, Z., Shao, C., Sun, W., and Zeng, Y. (2019) Differential urinary proteins to diagnose coronary heart disease based on iTRAQ quantitative proteomics. *Anal. Bioanal. Chem.* **411**, 2273–2282
27. Chauhan, M. Z., Valencia, A. K., Piqueras, M. C., Enriquez-Algeciras, M., and Bhattacharya, S. K. (2019) Optic nerve lipidomics reveal impaired glucosylsphingosine lipids pathway in glaucoma. *Invest. Ophthalmol. Vis. Sci.* **60**, 1789–1798
28. Egorov, V. V., Bachaldin, I. L., and Sorokin, E. L. (2001) [Characteristics of morphological and functional state of erythrocytes in patients with primary open-angle glaucoma with normalized intraocular pressure]. *Vestn. Oftalmol.* **117**, 5–8
29. Costet, P., Luo, Y., Wang, N., and Tall, A. R. (2000) Sterol-dependent transactivation of the ABC1 promoter by the liver X receptor/retinoid X receptor. *J. Biol. Chem.* **275**, 28240–28245
30. Son, J. H., Chung, Y. K., and Son, J. S. (2015) Apolipoprotein B: Novel indicator of elevated intraocular pressure. *Eye (Lond.)* **29**, 1315–1320
31. Mahley, R. W., Innerarity, T. L., Rall, S. C., Jr., and Weisgraber, K. H. (1984) Plasma lipoproteins: Apolipoprotein structure and function. *J. Lipid Res.* **25**, 1277–1294
32. Su, X., and Peng, D. (2020) The exchangeable apolipoproteins in lipid metabolism and obesity. *Clin. Chim. Acta* **503**, 128–135
33. Chen, H., Cho, K. S., Vu, T. H. K., Shen, C. H., Kaur, M., Chen, G., Mathew, R., McHam, M. L., Fazelat, A., Lashkari, K., Au, N. P. B., Tse, J. K. Y., Li, Y., Yu, H., Yang, L., *et al*. (2018) Commensal microflora-induced T cell responses mediate progressive neurodegeneration in glaucoma. *Nat. Commun.* **9**, 3209
34. Harder, J. M., Braine, C. E., Williams, P. A., Zhu, X., MacNicoll, K. H., Sousa, G. L., Buchanan, R. A., Smith, R. S., Libby, R. T., Howell, G. R., and John, S. W. M. (2017) Early immune responses are independent of RGC dysfunction in glaucoma with complement component C3 being protective. *Proc. Natl. Acad. Sci. U. S. A.* **114**, E3839–E3848
35. Liu, H., Anders, F., Funke, S., Mercieca, K., Grus, F., and Prokosch, V. (2020) Proteome alterations in aqueous humour of primary open angle glaucoma patients. *Int. J. Ophthalmol.* **13**, 176–179
36. Tsukamoto, H., Fukudome, K., Takao, S., Tsuneyoshi, N., and Kimoto, M. (2010) Lipopolysaccharide-binding protein-mediated Toll-like receptor 4 dimerization enables rapid signal transduction against lipopolysaccharide stimulation on membrane-associated CD14-expressing cells. *Int. Immunol.* **22**, 271–280
37. Zheng, M., Ambesi, A., and McKeown-Longo, P. J. (2020) Role of TLR4 receptor complex in the regulation of the innate immune response by fibronectin. *Cells* **9**, 216
38. McDonald, J. F., and Nelsestuen, G. L. (1997) Potent inhibition of terminal complement assembly by clusterin: Characterization of its impact on C9 polymerization. *Biochemistry* **36**, 7464–7473
39. Cooner, M., Mann, A., and Tighe, B. (2017) The nature and consequence of vitronectin interaction in the non-compromised contact lens wearing eye. *Cont. Lens Anterior Eye* **40**, 228–235
40. Almasieh, M., Wilson, A. M., Morquette, B., Cueva Vargas, J. L., and Di Polo, A. (2012) The molecular basis of retinal ganglion cell death in glaucoma. *Prog. Retin. Eye Res.* **31**, 152–181
41. Jacquot, J. P., de Lamotte, F., Fontecave, M., Schurmann, P., Decottignies, P., Miginiac-Maslow, M., and Wollman, E. (1990) Human thioredoxin reactivity-structure/function relationship. *Biochem. Biophys. Res. Commun.* **173**, 1375–1381
42. Mitchell, D. A., and Marletta, M. A. (2005) Thioredoxin catalyzes the S-nitrosation of the caspase-3 active site cysteine. *Nat. Chem. Biol.* **1**, 154–158
43. Langman, M. J., Lancashire, R. J., Cheng, K. K., and Stewart, P. M. (2005) Systemic hypertension and glaucoma: Mechanisms in common and co-occurrence. *Br. J. Ophthalmol.* **89**, 960–963
44. Duvesh, R., Puthuran, G., Srinivasan, K., Rengaraj, V., Krishnadas, S. R., Rajendrababu, S., Balakrishnan, V., Ramulu, P., and Sundaresan, P. (2017) Multiplex cytokine analysis of aqueous humor from the patients with chronic primary angle closure glaucoma. *Curr. Eye Res.* **42**, 1608–1613
45. Freedman, J., and Iserovich, P. (2013) Pro-inflammatory cytokines in glaucomatous aqueous and encysted Molteno implant blebs and their relationship to pressure. *Invest. Ophthalmol. Vis. Sci.* **54**, 4851–4855
46. Youngblood, H., Robinson, R., Sharma, A., and Sharma, S. (2019) Proteomic biomarkers of retinal inflammation in diabetic retinopathy. *Int. J. Mol. Sci.* **20**, 4755
47. Wang, J. W., Zhou, M. W., Zhang, X., Huang, W. B., Gao, X. B., Wang, W., Chen, S., Zhang, X. Y., Ding, X. Y., and Jonas, J. B. (2015) Short-term effect of intravitreal ranibizumab on intraocular concentrations of vascular endothelial growth factor-A and pigment epithelium-derived factor in neovascular glaucoma. *Clin. Exp. Ophthalmol.* **43**, 415–421
48. Ziff, J. L., Crompton, M., Powell, H. R., Lavy, J. A., Aldren, C. P., Steel, K. P., Saeed, S. R., and Dawson, S. J. (2016) Mutations and altered expression of SERPINF1 in patients with familial otosclerosis. *Hum. Mol. Genet.* **25**, 2393–2403
49. Ikeda, Y., Aihara, K., Yoshida, S., Iwase, T., Tajima, S., Izawa-Ishizawa, Y., Kihira, Y., Ishizawa, K., Tomita, S., Tsuchiya, K., Sata, M., Akaike, M., Kato, S., Matsumoto, T., and Tamaki, T. (2012) Heparin cofactor II, a serine protease inhibitor, promotes angiogenesis via activation of the AMP-activated protein kinase-endothelial nitric-oxide synthase signaling pathway. *J. Biol. Chem.* **287**, 34256–34263
50. Bury, S., Cichon, M., Bauchinger, U., and Sadowska, E. T. (2018) High oxidative stress despite low energy metabolism and vice versa: Insights through temperature acclimation in an ectotherm. *J. Therm. Biol.* **78**, 36–41
51. Wang, Y., Chen, S., Liu, Y., Huang, W., Li, X., and Zhang, X. (2018) Inflammatory cytokine profiles in eyes with primary angle-closure glaucoma. *Biosci. Rep.* **38**, BSR20181411
52. Clark, S. J., and Bishop, P. N. (2018) The eye as a complement dysregulation hotspot. *Semin. Immunopathol.* **40**, 65–74

53. Kasperska-Zajac, A., Grzanka, A., Machura, E., Misiolek, M., Mazur, B., and Jochem, J. (2013) Increased serum complement C3 and C4 concentrations and their relation to severity of chronic spontaneous urticaria and CRP concentration. *J. Inflamm. (London, England)* **10**, 22
54. Rao, G., Santhoshkumar, P., and Sharma, K. K. (2008) Anti-chaperone betaA3/A1(102-117) peptide interacting sites in human alphaB-crystallin. *Mol. Vis.* **14**, 666–674
55. Kurahashi, K., Inoue, S., Yoshida, S., Ikeda, Y., Morimoto, K., Uemoto, R., Ishikawa, K., Kondo, T., Yuasa, T., Endo, I., Miyake, M., Oyadomari, S., Matsumoto, T., Abe, M., Sakaue, H., *et al*. (2017) The role of heparin cofactor in the regulation of insulin sensitivity and maintenance of glucose homeostasis in humans and mice. *J. Atheroscler. Thromb.* **24**, 1215–1230
56. Vohra, R., and Kolko, M. (2018) Neuroprotection of the inner retina: Müller cells and lactate. *Neural Regen. Res.* **13**, 1741–1742
57. Vohra, R., Aldana, B. I., Skytt, D. M., Freude, K., Waagepetersen, H., Bergersen, L. H., and Kolko, M. (2018) Essential roles of lactate in Müller cell survival and function. *Mol. Neurobiol.* **55**, 9108–9121
58. Sun, X., Dai, Y., Chen, Y., Yu, D. Y., Cringle, S. J., Chen, J., Kong, X., Wang, X., and Jiang, C. (2017) Primary angle closure glaucoma: What we know and what we don't know. *Prog. Retin. Eye Res.* **57**, 26–45
59. Gassel, C. J., Reinehr, S., Gomes, S. C., Dick, H. B., and Joachim, S. C. (2020) Preservation of optic nerve structure by complement inhibition in experimental glaucoma. *Cell Tissue Res.* **382**, 293–306